© 2014. Published by The Company of Biologists Ltd | Development (2014) 141, 830-841 doi:10.1242/dev.104687

RESEARCH ARTICLE

STEM CELLS AND REGENERATION

The ERECTA receptor kinase regulates *Arabidopsis* shoot apical meristem size, phyllotaxy and floral meristem identity

Tali Mandel[1], Fanny Moreau[2], Yaarit Kutsher[1], Jennifer C. Fletcher[3], Cristel C. Carles[2] and Leor Eshed Williams[1,*]

ABSTRACT

In plants, the shoot apical meristem (SAM) serves as a reservoir of pluripotent stem cells from which all above ground organs originate. To sustain proper growth, the SAM must maintain homeostasis between the self-renewal of pluripotent stem cells and cell recruitment for lateral organ formation. At the core of the network that regulates this homeostasis in *Arabidopsis* are the WUSCHEL (WUS) transcription factor specifying stem cell fate and the CLAVATA (CLV) ligand-receptor system limiting *WUS* expression. In this study, we identified the ERECTA (ER) pathway as a second receptor kinase signaling pathway that regulates *WUS* expression, and therefore shoot apical and floral meristem size, independently of the CLV pathway. We demonstrate that reduction in class III HD-ZIP and ER function together leads to a significant increase in *WUS* expression, resulting in extremely enlarged shoot meristems and a switch from spiral to whorled vegetative phyllotaxy. We further show that strong upregulation of *WUS* in the inflorescence meristem leads to ectopic expression of the *AGAMOUS* homeotic gene to a level that switches cell fate from floral meristem founder cell to carpel founder cell, suggesting an indirect role for ER in regulating floral meristem identity. This work illustrates the delicate balance between stem cell specification and differentiation in the meristem and shows that a shift in this balance leads to abnormal phyllotaxy and to altered reproductive cell fate.

KEY WORDS: AGAMOUS (AG), Cell fate, WUSCHEL (WUS)

INTRODUCTION

In higher plants, all the aerial organs are produced post-embryonically through the activity of a pluripotent stem cell reservoir that resides in the apex of the meristem at the shoot tip (Carles and Fletcher, 2003; Sablowski, 2004). These cells divide slowly to renew themselves and to supply cells to the interior or to the periphery of the shoot apical meristem (SAM), where their progeny divide more rapidly to provide cells for the stem and for lateral organ primordia (Williams and Fletcher, 2005). The ability of the SAM to produce lateral organs while maintaining the appropriate size requires tightly controlled balance between cell proliferation in the central zone (CZ) and cell recruitment for primordium initiation in the peripheral zone (PZ) (Clark et al., 1997; Golz and Hudson, 2002; Wahl et al., 2010). Therefore, plants have evolved a complex genetic network that controls SAM size. At the core of this network is the WUSCHEL (WUS) transcription factor, which specifies the pluripotent state in the CZ, and the CLAVATA (CLV) ligand-receptor system that limits *WUS* expression to maintain a stable stem cell population size (Brand et al., 2000; Carles and Fletcher, 2003; Schoof et al., 2000). This negative-feedback loop is further fine-tuned by many other signaling pathways and molecular mechanisms such as epigenetic factors and other receptor systems (Perales and Reddy, 2012). Extensive genetic screens have identified numerous mutants with abnormal shoot and/or floral meristem size, uncovering many genes that participate in the regulation of meristem size and function (DeYoung et al., 2006; Fletcher, 2001; Furner and Pumfrey, 1992; Kaya et al., 2001; Laux et al., 1996; Long and Barton, 1998; Vidaurre et al., 2007; Wu et al., 2005). Nevertheless, some genes may act in partially redundant parallel pathways and therefore have not yet been uncovered.

Redundancy in SAM regulation is illustrated by the three members of the *Arabidopsis ERECTA* (*ER*) gene family that encode leucine-rich-repeat receptor kinases (Torii et al., 1996), which are broadly expressed and play redundant roles in diverse aspects of plant development (Shpak et al., 2004; Uchida et al., 2012; Yokoyama et al., 1998). Mutations in the *ER* gene enhance the SAM phenotypes of other mutants (Durbak and Tax, 2011; Uchida et al., 2011), and it has been suggested that the ER family regulates meristem homeostasis by buffering cytokinin responsiveness in the SAM (Uchida et al., 2013).

In the SAM peripheral zone, leaves initiate with a regular spacing that determines the phyllotaxis (Sussex, 1998; Traas, 2013). An accepted model for phyllotaxis regulation is that high auxin level accumulation at a precise position in the PZ triggers organ initiation. Local auxin maxima are achieved by auxin polar transporters that actively deplete the auxin from nearby cells (Vieten et al., 2007), resulting in low concentrations in the vicinity of the existing organ primordia. This allows a new auxin maximum, and therefore a new organ primordium, to develop only at a specific minimum distance from the pre-existing primordia (Jönsson et al., 2006; Lohmann et al., 2010; Smith et al., 2006).

Once the SAM switches from vegetative to reproductive phase, lateral organ identity changes and the inflorescence meristem (IM) produces floral meristems (FM) on its flanks. Each FM provides all the cells to form the four whorls of floral organs – sepals, petals, stamens and carpels – before ceasing its meristematic activity. The identity of each floral organ is specified by different combinations of transcription factors encoded by several classes of genes that form the basis for the ABCE[D] model of flower development (Bowman et al., 2012; Krizek and Fletcher, 2005). In *Arabidopsis*, the C-class floral homeotic gene *AGAMOUS* (*AG*) is expressed in the center of the FM and specifies carpel identity in whorl four, while also acting

[1]The Robert H. Smith Faculty of Agriculture, Food and Environment, The Hebrew University of Jerusalem, POB 12 Rehovot 76100, Israel. [2]CNRS, UMR5168, F-38054 Grenoble, France. [3]Plant Gene Expression Center, USDA–ARS/University of California, Berkeley, 800 Buchanan Street, Albany, CA 94710, USA.

*Author for correspondence (leor.williams@mail.huji.ac.il)

This is an Open Access article distributed under the terms of the Creative Commons Attribution License (http://creativecommons.org/licenses/by/3.0), which permits unrestricted use, distribution and reproduction in any medium provided that the original work is properly attributed.

Received 23 October 2013; Accepted 8 December 2013

Development (2014) doi:10.1242/dev.104687

with B-class genes to specify stamen identity in whorl three (Coen and Meyerowitz, 1991). During wild-type flower development, *WUS* is expressed in stage 1 floral primordia (stages according to Smyth et al., 1990) and is repressed once the carpel primordia form at stage 6, which results in FM termination (Lenhard et al., 2001). WUS binds directly to the second intron of *AG* and together with the LEAFY transcription factor, activates *AG* expression at floral stage 3 (Busch et al., 1999).

We have previously reported on the role of the *Arabidopsis* microRNA *miR166g* in regulating *WUS*-dependent SAM activity (Williams et al., 2005). We demonstrated that in *jabba-1D* (*jba-1D*) plants, overexpression of *miR166g* causes a decrease in the transcript levels of several class III homeodomain-leucine-zipper (*HD-ZIPIII*) target genes, which leads to a dramatic increase in *WUS* transcript levels and expansion of its expression domain, resulting in SAM enlargement (Williams et al., 2005).

To uncover novel genes that act redundantly with the *HD-ZIPIII* pathway in meristem regulation, we conducted a genetic screen to identify second-site mutations that modified the *jba-1D* enlarged SAM phenotypes and identified a mutation in the *ER* gene as an enhancer. *jba-1D* plants carrying the mutated ER modifier exhibit extremely enlarged SAMs with altered leaf phyllotaxis and ectopic carpels forming directly from the inflorescence meristem. We demonstrate that, owing to aberrant ER function, the *WUS* gene is upregulated, leading to ectopic *AG* expression and subsequent ectopic carpel formation. Our results indicate that the *ER* gene regulates SAM size in a genetic pathway parallel to those of the *HD-ZIPIII* and *CLV* pathways, and that ER has a similar function in the floral meristem, where it plays a role in regulating meristem size and homeostasis.

RESULTS

A mutation in the *ERECTA* gene enhances the *jba-1D/+* enlarged meristem phenotype

Arabidopsis jba-1D plants display pleiotropic developmental phenotypes, in which the most prominently is a dramatic enlargement of the SAM that results in extremely fasciated stems and enlarged IMs that produce many extra flowers (Williams et al., 2005) (supplementary material Fig. S1). These phenotypes are caused by dosage-dependent upregulation of *miR166g*. To identify other genes involved in SAM regulation, we performed a genetic modifier screen of ethyl methanesulfonate (EMS) mutagenized *jba-1D/+* plants. We identified a strong modifier exhibiting meristem-related phenotypes that we termed *jabba Modifier1* (*jM1*). The *jM1* mutant was backcrossed twice into the *jba-1D/+* parental background and the modifier was shown to act as a single nuclear trait.

jM1 homozygous single mutant plants display round leaves with short petioles and a compact inflorescence with flowers clustering at the top (supplementary material Fig. S2). This phenotype closely resembles those of Landsberg *erecta* (L*er*) plants (Torii et al., 1996), although *jM1* plants are in the Col-0 genetic background. This resemblance led us to investigate whether the modifier mutation in *jM1* was in the *ER* gene. Sequencing the *ER* gene from *jM1* individuals confirmed the presence of a missense mutation that causes an isoleucine to threonine substitution at amino acid 750 in the cytoplasmic serine/threonine protein kinase domain (Lease et al., 2001). We performed a complementation assay (supplementary material Fig. S3), demonstrating that the missense mutation in the *ER* gene causes the strong enhancement of the *jba-1D/+* phenotype. We therefore named this recessive allele *er-20*.

Analysis of *jba-1D/+er-20* plants revealed two distinct morphological phenotypes (Figs 1, 3). At the vegetative stage, *jba-1D/+er-20* seedlings lack the typical spiral phyllotaxis displayed by wild-type and *jba-1D/+* seedlings (Fig. 1A-C,H,I), and the SAMs of *jba-1D/+er-20* plants show additional enlargement relative to *jba-1D/+* plants (Fig. 1J-L). In wild-type and *jba-1D/+* seedlings (Fig. 1A-C), the first pair of true rosette leaves emerges simultaneously in a decussate pattern, and all subsequent leaves arise following a spiral phyllotaxy characterized by the ‘golden angle’ of about 137.5°. Sixteen-day-old *jba-1D er-20* seedlings exhibit similar phenotype to *jba-1D* seedlings in their first two radial leaves and successive curled leaves, although somewhat more severe (Fig. 1D,F). By contrast, *jba-1D/+er-20* seedlings exhibit a decussate pattern for the first pair of leaves followed by a transition to a whorled phyllotaxis (Fig. 1H,I). Four rosette leaves arise at the same time in an iterative manner throughout the vegetative phase, as do the cauline leaves (supplementary material Fig. S1). We examined the leaf primordia initiation by performing scanning electron microscopy (SEM) on *jba-1D/+er-20* seedlings and found that the four primordia emerge simultaneously at the SAM periphery (Fig. 1G), suggesting the concurrent establishment of auxin maxima at four distinct locations around the SAM (Fig. 1N).

Next, we examined at the histological level the SAM of wild-type, *jba-1D/+* and *jba-1D/+er-20* plants. Sections through 9-day-old

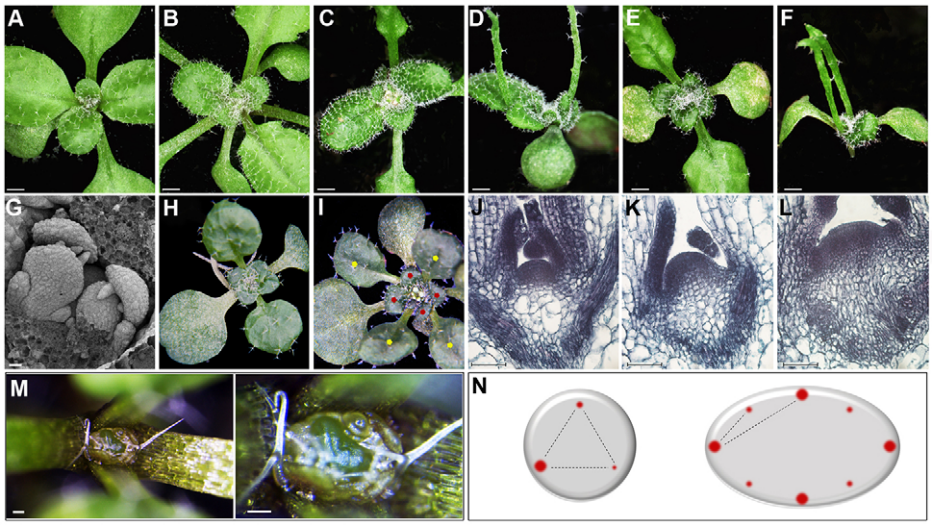

Fig. 1. The *jba-1D/+er-20* SAM is enlarged and shows altered phyllotactic patterning. (A-F) Sixteen-day-old seedlings. (A) L*er*, (B) Col, (C) *jba-1D/+*, (D) *jba-1D*, (E) *jba-1D/+er-20* and (F) *jba-1D er-20*. (G) SEM of *jba-1D/+er-20* seedling showing four leaf primordia emerging from the SAM. (H,I) *jba-1D/+er-20* seedlings with four leaves arising simultaneously in concentric whorls, the first four marked with yellow and the next four with red. (J-L) Longitudinal sections of 9-day-old seedlings. (J) Col. (K) *jba-1D/+*. (L) *jba-1D/+er-20* and (M) *jba-1D/+er-20* vegetative SAM at two different magnifications. (N) Schematic diagram of auxin maxima (red dots) at leaf primordia initiation sites in meristems of two different sizes. Scale bars: 1 mm in A-E; 200 μm in G; 50 μm in J-L; 100 μm in M.

Development (2014) doi:10.1242/dev.104687

seedlings revealed that the *er-20* mutation enhances the *jba-1D/+* enlarged SAM phenotype (Fig. 1K) leading to an extremely enlarged meristem (Fig. 1L). In some cases, the huge meristem can be seen easily with the naked eye (Fig. 1M). The *jba-1D/+er-20* SAM enlargement and its altered phyllotaxis are consistent with reports showing that altered SAM size can lead to changes in phyllotaxis (Clark et al., 1993; Giulini et al., 2004; Laufs et al., 1998a; Medford et al., 1992; Leyser and Furner, 1992; Takahashi et al., 2002).

To further test the hypothesis that meristem enlargement is accompanied by simultaneous establishment of several auxin maxima (Fig. 1N), we performed RT-qPCR on 8-day-old whole seedlings using gene specific primers for *SHOOT MERISTEMLESS* (*STM*) and *GH3.3* (Fig. 2). *STM* encodes a class I KNOX transcription factor that is expressed throughout the SAM and promotes meristem cell proliferation (Long et al., 1996). The *GH3.3* gene is an early auxin-responsive gene that is expressed during primordium initiation, from the first sign of cell bulging at the SAM periphery to leaf plastochron 4 (Efroni et al., 2008; Mallory et al., 2005). The results showed an approximately twofold increase in *STM* expression levels in *jba-1D/+er-20* compared with *jba-1D/+* seedlings, consistent with the meristem enlargement phenotype (Fig. 1L). The moderate increase in *STM* levels reflects the small fraction of meristematic cells within the whole seedling samples. With a higher proportion of meristematic cells in *jba-1D/+er-20*, we would expect a reduction in *GH3.3* transcript levels due to dilution of the *GH3.3*-expressing primordia cells within the whole seedlings. Yet RT-qPCR analysis showed an approximately twofold increase in *GH3.3* expression in *jba-1D/+er-20* plants (Fig. 2). This indicates that the *jba-1D/+er-20* SAM contains more cells expressing the early auxin-responsive *GH3.3* gene, consistent with the formation of additional auxin maxima for organ initiation. Our results therefore indicate that ER restricts SAM size during vegetative development, and that restricting SAM size may prevent the production of more than one auxin maximum at a time.

It has recently been suggested that the SAM possesses a functional buffering mechanism regulated by the ER receptor kinase family to maintain CLV3 homeostasis regardless of an increase in *WUS* expression induced by cytokinin treatment (Uchida et al., 2013). We therefore assessed the *WUS* and *CLV3* expression levels by RT-qPCR. We observed a dramatic increase in *WUS* expression in *jba-1D/+er-20* compared with *jba-1D/+* seedlings, whereas *CLV3* expression levels were not significantly different (Fig. 2). In the absence of functional ER we would expect increased levels of *CLV3* transcripts because of the increase in *WUS* expression. Therefore, this result raises the possibility that the *jba-1D/+er-20* meristem contains more cells of all types and that the ratio between the whole meristem tissue and the *CLV3*-expressing stem cells is maintained.

To test whether other ER family members compensate for the mutation in *ER*, we analyzed the expression of *ER*, *ERECTA LIKE 1* and *ERECTA LIKE 2* (*ERL1* and *ERL2*). We found no differential expression for *ER* and *ERL1* but a 1.7-fold increase in *ERL2* expression levels in *jba-1D/+er-20* relative to *jba-1D/+* plants. These results are consistent with the view that *ER* genes redundantly regulate the vegetative SAM (Uchida et al., 2013) and imply that

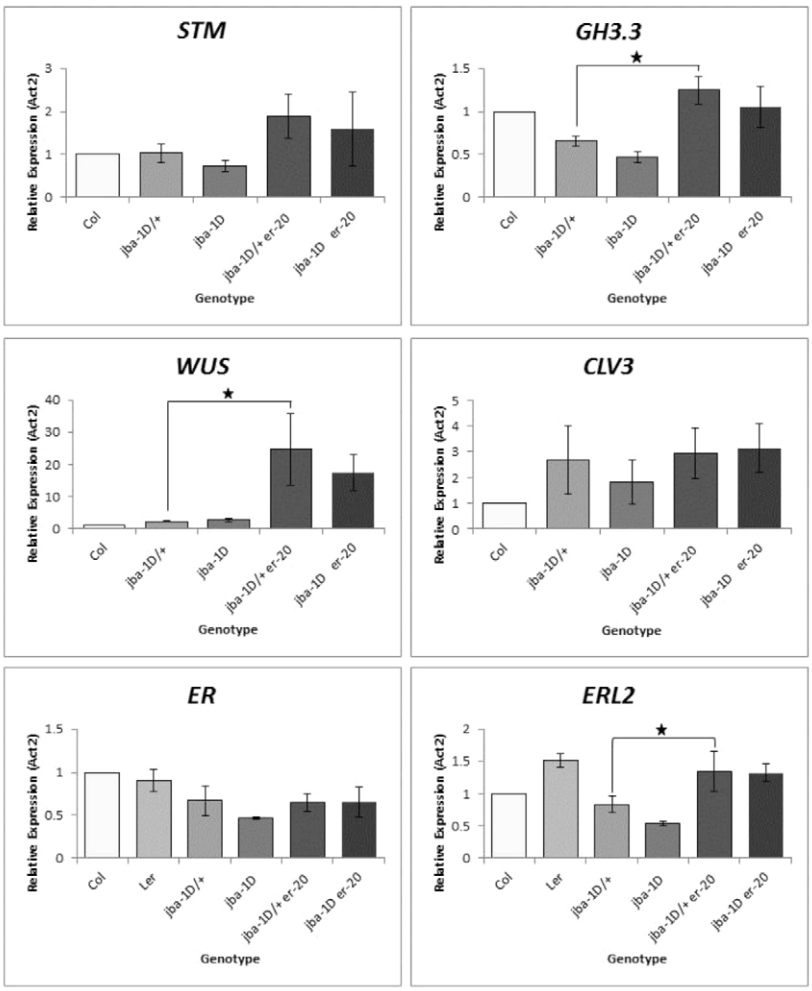

Fig. 2. Relative transcript levels of *STM*, *GH3.3*, *WUS*, *CLV3*, *ER* and *ERL2* in wild-type and mutant seedlings. Relative transcript levels (mean±s.e.m.) were calculated from triplicate RT-qPCR reactions of independent RNA samples prepared from three different sets of 8-day-old *Arabidopsis* seedlings. The transcript levels in Col are set to 1. Relative expression is normalized to *ACTIN2*. Asterisks indicate statistical significance (P<0.05, n=3).

Development (2014) doi:10.1242/dev.104687

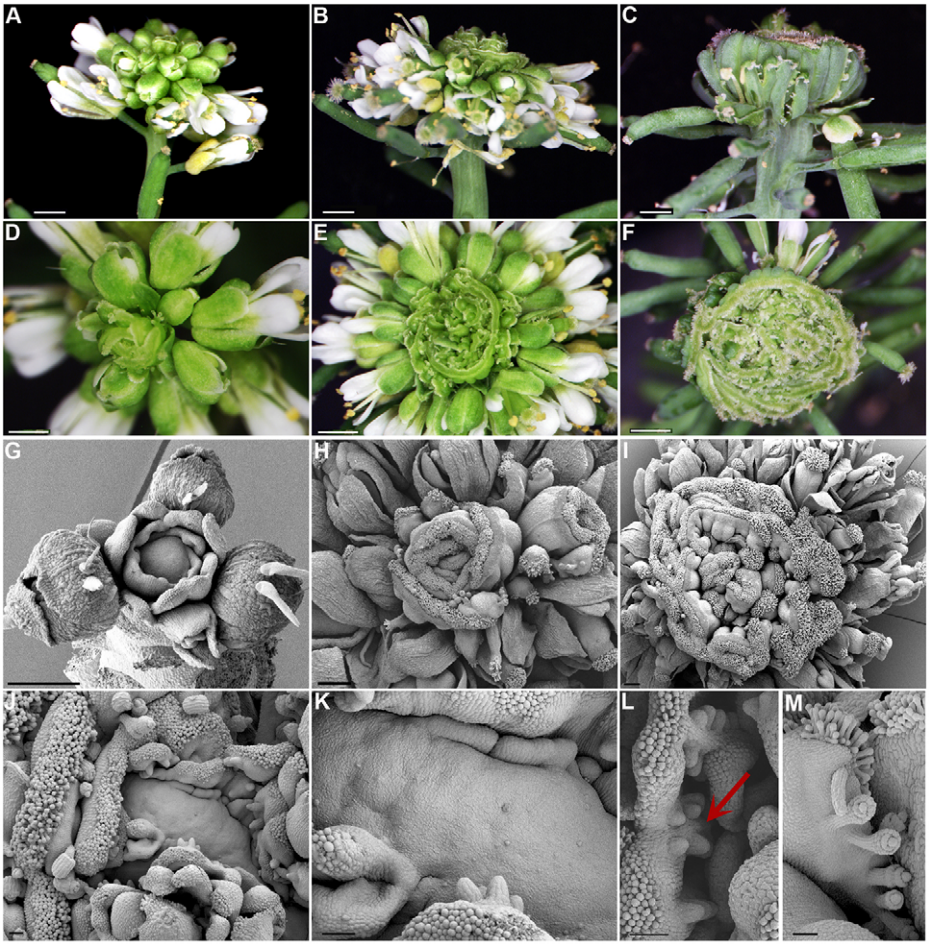

Fig. 3. *jba-1D/+er-20* IMs ectopically produce multiple fused carpels. (A-F) Side and top views of progressively older *jba-1D/+er-20* inflorescence. (A,D) Young inflorescence. (B,E) Older inflorescence with whorls of ectopic fused carpels. (C,F) Severely fasciated inflorescence displaying multiple whorls of ectopic fused carpels. (G-M) Scanning electron microscopy of progressively older *jba-1D/+er-20* IMs. (G) Young dome-shaped IM with carpels beginning to form around the flanks. (H,I) Older IMs with multi-fused carpels consisting of distinctive valves, replum, style and stigma. (J) Unfused multi-carpel gynoecia. (K) Extremely enlarged IM with ectopic carpels developing directly from the SAM flanks. (L) Developing ovule primordia projecting on the opposing placenta (red arrows). (M) A mature unfused ectopic gynoecium with multiple ovules. Scale bars: 2 mm in A-I; 200 µm in J-M.

ERL2 upregulation compensates for the mutation in *ER* in maintaining *CLV3* homeostasis.

jba-1D/+ er-20 inflorescence meristems ectopically produce multi-fused carpels

During reproductive development, mature *jba-1D/+er-20* plants form ectopic, multi-fused carpels around the IM (Fig. 3). Like *jba-1D* plants, *jba-1D/+er-20* form fasciated IMs that produce numerous flowers (Fig. 3A). However, 4-5 weeks after bolting, the inflorescence starts to form carpels at the periphery in place of complete flowers (Fig. 3A,D). Initially, a single or a few fused carpels emerge in a spiral phyllotaxy around the inflorescence (Fig. 3D) and the structures gradually develop as multi-fused carpels that encircle the IM almost as one piece (Fig. 3B,C,E,F). Iterations of whorls of ectopic multi-carpels form internal to one another, ultimately resulting in a massive structure of carpels within carpels at the top of the inflorescence stem (Fig. 3C,F; supplementary material Fig. S4C). The IM continues to produce carpels even 16 weeks after bolting, after the rest of the plant has senesced (supplementary material Fig. S5).

In *Arabidopsis*, each flower primordium initiates at the IM periphery as a small bulge of cells that divide and expand in three dimensions, generating a hemispherical primordium that becomes separated from the IM by a small groove (Kwiatkowska, 2006; Smyth et al., 1990). This primordium represents a *de novo* FM from which the four types of floral organs will arise in concentric rings called whorls. To determine whether the *jba-1D/+er-20* ectopic carpels develop from FMs or arise directly from the IM, we performed SEM analysis (Fig. 3G-M). Initially, the *jba-1D/+er-20* IM develops normal flowers, until a sharp transition to the formation of carpels as lateral organs occurs (Fig. 3G). Each carpel primordium arises directly from the meristem as a bulge on its edge that gradually becomes delineated from the IM (Fig. 3G,J,K; supplementary material Fig. S4A). We conclude that the ectopic carpels initiate directly from the *jba-1D/+er-20* IM, indicating a change in cell identity from FM fate to carpel fate at the IM periphery.

The wild-type *Arabidopsis* gynoecium initiates as a raised rim around the center of the FM that grows and forms a hollow cylinder (Alvarez-Buylla et al., 2010). Very rarely the *jba-1D/+er-20* inflorescence forms typical cylindrical gynoecium structures in the center of the huge IM, in addition to ectopic carpels on the flanks (supplementary material Fig. S4B). All the ectopic carpels on the *jba-1D/+er-20* IM consist entirely of carpel-specific tissues, but they fail to form an open-ended tube that will fuse to generate the seed-bearing ovaries of a mature gynoecium. In each ectopic carpel, a valve flanked with valve margin, style bearing stigmatic papillae, replum and septum tissues are visible (Fig. 3H,I,L,M; supplementary material Fig. S4C). The adaxial side of the fused carpels shows reduced septum tissues with two rows of ovule primordia growing on opposite sides (Fig. 3L) and in the unfused mature gynoecium the ovule funiculus, inner and outer integuments are observed (Fig. 3M).

In summary, these observations indicate that *miR166g* overexpression and aberrant *ER* function in *jba-1D/+er-20* plants lead to an extreme IM enlargement and to the formation of ectopic carpel structures in place of functional FMs. Therefore, *miR166g*

Development (2014) doi:10.1242/dev.104687

and ER function are together required to restrict IM size and specify floral meristem identity.

Many gynoecium development genes are upregulated in *jba-1D/+ er-20* IMs

To further explore the hypothesis that *jba-1D/+ er-20* IMs develop carpels on the periphery due to a switch in cell identity, we carried out an RNA-Seq analysis on *jba-1D/+* and *jba-1D/+ er-20* IMs. We collected 30 dissected inflorescences from each genotype at 4 weeks after bolting, once the first plant began to exhibit ectopic carpel formation. All the flowers were removed, leaving either bare meristems with undetachable primordia for *jba-1D/+* IMs, or bare meristems with a mixture of un-detachable floral and carpel primordia for *jba-1D/+ er-20* IMs. The meristems were independently pooled for mRNA isolation, sequencing and differential expression analysis (supplementary material Table S1).

As expected, *WUS* expression levels are fourfold higher in *jba-1D/+ er-20* IMs compared with *jba-1D/+* IMs, even though in *jba-1D/+* the remaining floral primordia on the IMs contributed to the total *WUS* transcript levels, whereas in *jba-1D/+ er-20* the source was mainly cells from the IMs themselves. This result indicates a much higher level of *WUS* expression in *jba-1D/+ er-20* IMs, and demonstrates that ER negatively regulates *WUS* in the IM. As in the vegetative SAM, the *GH3.3* gene is upregulated in *jba-1D/+ er-20* IMs (Table 1), again suggesting the occurrence of additional auxin maxima around the IM. For the *ER* genes, although *ER* and *ERL2* are not differentially expressed, *ERL1* expression levels were threefold higher in *jba-1D/+ er-20* IMs.

In addition, many of the CE[D] class floral organ identity genes are upregulated in *jba-1D/+ er-20* plants (Table 1). For example, carpels are specified by the class C MADS-box gene *AG*, along with the related *SHATTERPROOF1* (*SHP1*), *SHP2* and *SEEDSTICK* (*STK*) genes (Becker and Theissen, 2003; Pinyopich et al., 2003). *STK* also acts redundantly with *SHP1* and *SHP2* to promote ovule identity determination (Colombo et al., 2010). Because ectopic carpels develop directly from the *jba-1D/+ er-20* IMs, we expected these four genes to be highly expressed. Indeed, *AG* and *SHP1* are both upregulated sevenfold in *jba-1D/+ er-20* compared with *jba-1D/+* IMs, *SHP2* is elevated 65-fold, and *STK* is elevated 40-fold (Table 1). In addition, three *SEPALLATA* (*SEP*) genes that function redundantly as class E genes are upregulated in *jba-1D/+ er-20* IMs: *SEP1* by fourfold, *SEP2* by threefold and *SEP3* by 2.8-fold. The AG transcription factor orchestrates the expression of numerous downstream genes (Gómez-Mena et al., 2005; Ito et al., 2007; Ito et al., 2004). We found that many AG immediate targets and directly bound genes are upregulated in *jba-1D/+ er-20* IMs, including *CRC*, *SEP3* and *SHP1* (Gómez-Mena et al., 2005) (supplementary material Table S2). In summary, many early gynoecium specification genes are upregulated in *jba-1D/+ er-20* plants.

Together, our morphological and molecular datasets indicate that the *ER* gene is required to constrain *WUS* mRNA expression in *jba-1D/+* meristems. We also find that it limits the transcription levels of floral organ identity genes, such as *AG*. We propose that in *jba-1D/+ er-20* IMs, high levels of *WUS* transcripts lead to ectopic activation of *AG* expression. At the IM periphery, where the cells are competent to develop into flowers, this ectopic *AG* expression activates its downstream genes, leading to a switch in cell identity and the initiation of carpel formation.

jba-1D/+ er-20 IMs show ectopic expression of *WUS* and *AG*

In *jba-1D/+ er-20* plants, the vegetative SAM and IM exhibit elevated levels of *WUS* expression, indicating that ER negatively regulates *WUS*. Yet, it is unclear whether ER tunes *WUS* transcription levels or limits its expression domain. To analyze this, we performed RNA *in situ* hybridization with a *WUS* probe (Fig. 4). In wild-type Col IMs, *WUS* is expressed in the central cells of the IM and the FM, a region termed the organizing center (OC) (Fig. 4A). In *jba-1D/+* IMs, the *WUS* expression pattern is similar to that of *clv3-2* IMs (Fig. 4B), in which the domain expands laterally and upward into the outermost two to three layers across the meristem (Brand et al., 2000). In *jba-1D/+ er-20* IMs, not only is the *WUS* signal is more intense than in *jba-1D/+* IMs, it expands further into the interior cell layers (Fig. 4C). Thus, ER is a regulator that contributes both to limiting *WUS* transcript levels and to restricting the *WUS* expression domain to the OC. We have previously reported that *wus-1 jba-1D* meristems are indistinguishable from *wus-1* meristems (Williams et al., 2005), indicating that WUS activity is absolutely required to obtain the *jba* SAM phenotypes. As *wus-1* suppresses the *jba-1D/+* phenotypes, it will also suppress the *jba-1D/+ er-20* phenotypes, as *er-20* single mutants do not exhibit ectopic carpel formation.

To further investigate the hypothesis that ectopic *AG* expression can lead to a switch in cell identity at the IM periphery, we tested whether ectopic *AG* expression accompanies the initiation of ectopic carpels in *jba-1D/+ er-20* IMs using RNA *in situ* hybridization. In wild-type plants, *AG* mRNA is absent from the IM but is first detected in the center of stage 3 floral primordia prior to stamen and carpel initiation (Fig. 4D,E,H). *AG* expression is later confined to the inner two whorls of the flower. At stage 9, *AG* mRNA is detected at low levels in the valves of the developing carpels and at high levels in ovule primordia (Drews et al., 1991; Ito et al., 2004; Yanofsky et al., 1990). *AG* expression is unaltered in *jba-1D/+* floral primordia, but unexpectedly we also detect a faint signal in the L1, L2 and uppermost L3 cell layers across the IM (Fig. 4F,G), indicating that *AG* is ectopically expressed in *jba-1D/+* IMs. However, in *jba-1D/+* L*er* and *jba-1D/+ er-20* IMs, *AG* expression is much more intense in the outer cell layers (Fig. 4I-M) than in *jba-1D/+* IMs, and spreads to more layers inwards. Furthermore, *jba-1D/+ er-20* ectopic carpels show strong *AG* expression on their adaxial side and in ovule primordia (Fig. 4K,M). These results are consistent with our proposed scenario that strong ectopic *AG* expression at the IM periphery leads to a cell identity switch from flower founder cell identity to carpel cell identity.

Next, we tested whether *AG* is required for the ectopic carpel phenotype by crossing *jba-1D/+ er-20* to *ag-1*-null mutant plants. The stems of *jba-1D/+ er-20 ag-1* plants are extremely fasciated and the IMs develop flowers lacking stamens and carpels (Fig. 5K,L). However, the IMs never generate ectopic carpel structures on their flanks, even late in their life cycles (Fig. 5K,L), indicating that *AG* is required to confer the *jba-1D/+ er-20* ectopic carpel phenotype.

Effect of *ER* gene family mutations on the *jba-1D/+* phenotype

To determine whether other mutations in *ER* could generate phenotypes like those of *jba-1D/+ er-20* plants, we analyzed the genetic interactions between *jba-1D/+* and either the L*er* accession or the Col accession carrying the *er-2* allele. L*er* contains a point mutation in the *ER* kinase domain (Torii et al., 1996) and is likely to be a null allele (Lease et al., 2001). *jba-1D/+* L*er* plants display two types of phenotypes. The first is a less severe version of the *jba-1D/+ er-20* carpel phenotype, where ectopic carpel formation ceases as the plants senesce (Fig. 5A,B). The second is the formation of a macroscopic IM with several whorls of ectopic carpels that encircle the IM but do not form reiterative multi-fused carpels structures

Development (2014) doi:10.1242/dev.104687

Table 1. Selected upregulated genes in *jba-1D/+er-20* compared with *jba-1D/+* IMs

AGI	Gene annotation/description	*jba+/−* (RPKM)	*jba-1D/+ er-20* (RPKM)	Fold change
AT2G21650	*MATERNAL EFFECT EMBRYO ARREST 3, MEE3* (involved during early morphogenesis)	0.03	15.5	512
AT5G09750	*HEC3, AGL5* (involved in transmitting tissue development, carpel formation, regulation of transcription)	0.17	41	223
AT2G01500	*WUSCHEL RELATED HOMEOBOX, WOX6* (gene that delays differentiation and maturation of primordia and regulates ovule patterning)	0.03	6.3	194
AT2G21450	*CHROMATIN REMODELING 34, CHR34*	0.34	9.78	28
AT1G25330	*CES*, *CESTA* (a positive regulator of brassinosteroid biosynthesis)	0.28	22.4	78
AT2G42830	*SHATTERPROOF 2, SHP2, AGL5* (involved in fruit development and a putative direct target of AG)	0.54	35.7	65
AT5G65080	*AGL68* (regulates flowering time)	0.22	13.3	56
AT4G09960	*AGL11, STK* (TF expressed in the carpel and ovules)	0.24	46	40
AT2G33880	*WUSCHEL RELATED HOMEOBOX, WOX9, STIP* (required for meristem growth and development and acts through positive regulation of WUS)	1.93	75.5	39
AT3G62820	Plant invertase/pectin methylesterase inhibitor superfamily protein	1.9	49.4	26
AT5G18000	*VERDANDI, VDD* (a direct target of the MADS domain ovule identity complex)	0.78	17.3	22
AT5G23260	*AGAMOUS-LIKE 32, AGL32* (shown to be necessary for determining the identity of the endothelial layer within the ovule)	0.09	2.15	23
AT3G50330	*HEC2* (involved in ovary septum development, transmitting tissue development, carpel formation, regulation of transcription)	0.89	15.3	17
AT5G21150	*ARGONAUTE 9* (AGO9-dependent sRNA silencing is crucial to specify cell fate in the *Arabidopsis* ovule)	5.98	98.6	16
AT5G41410	*BELL 1* (homeodomain protein required for ovule identity)	0.83	12.5	15
AT2G26440	Plant invertase/pectin methylesterase inhibitor superfamily	5.5	53.7	
AT3G51060	*STYLISH 1* (promotes gynoecium, stamen and leaf development)	1.2	11.3	9
AT1G23420	*INNER NO OUTER, INO* (may be required for polarity determination in the central part of the ovule)	0	5.4	5
AT4G18960	*AGAMOUS, AG* (specifies floral meristem and carpel and stamen identity)	9.4	70	7
AT3G58780	*SHATTERPROOF 1, SHP1* (required for fruit dehiscence. Controls dehiscence zone differentiation)	7.2	49	7
AT1G69180	*CRABS CLAW, CRC* (putative TF involved in specifying abaxial cell fate in the carpel)	22	142.3	7
AT3G18010	*WUSCHEL RELATED HOMEOBOX, WOX1* (encodes a WUSCHEL-related homeobox gene family member)	1.78	10.7	6
AT1G66350	*RGL1* (negative regulator of GA responses, member of GRAS family of transcription factors; involved in flower and fruit development)	10.5	53	5
AT3G23130	*SUPERMAN, SUP* (flower-specific gene controlling the boundary of the stamen and carpel whorls)	2.15	9.25	5
AT3G22880	*ARLIM15* (expression is restricted to pollen mother cells in anthers and to megaspore mother cells in ovules)	6.5	28.3	5
AT5G15800	*SEPALLATA1, SEP1* (encodes a MADS box transcription factor involved flower and ovule development)	22.3	96	4
AT5G11320	*YUCCA4, YUC4* (belongs to the YUC gene family. Involved in auxin biosynthesis and plant development)	2.2	8.8	4
AT3G57670	*NO TRANSMITTING TRACT, NTT* (TF specifically expressed in the transmitting tract and involved in transmitting tract development and pollen tube growth)	4.9	19.8	4
AT2G17950	*WUSCHEL, WUS* (homeobox gene controlling the stem cell pool; required to keep the stem cells in an undifferentiated state)	1.2	4.9	4
AT1G24260	*SEPALLATA3, SEP3* (member of the MADs box transcription factor family; SEP3 is redundant with SEP1 and 2)	28.7	103.7	4
AT5G66350	*SHORT INTERNODES, SHI* (function synergistically with other SHI-related genes promote gynoecium, stamen and leaf development)	1.8	5.8	3.3
AT5G62230	*ERECTA-LIKE 1, ERL1* (encodes a receptor-like kinase; along with *ERL2* functionally compensates for loss of ER during integument development)	16.6	48.2	3
AT4G36920	*APETALA 2, AP2* (involved in the specification of floral organ identity, establishment of floral meristem identity, suppression of floral meristem indeterminancy, and development of the ovule and seed coat)	7.7	29.9	3.9
AT2G23170	*GH3.3* (encodes an IAA-amido synthase that conjugates Asp and other amino acids to auxin *in vitro*)	10.6	26.7	2.5
AT5G17810	*WUSCHEL RELATED HOMEOBOX, WOX12* (encodes *WUSCHEL RELATED HOMEOBOX* gene family member with 65 amino acids in its homeodomain)	2.8	9.7	3.5
AT3G02310	*SEPALLATA 2, SEP2* (MADS-box protein, binds K domain of AG *in vivo*)	56.6	155.7	2.8
AT1G68640	*PERIANTHIA, PAN* (encodes bZIP-transcription factor, and is essential for AG activation in early flowers of short-day-grown plants)	15.1	32	2

Gene names and descriptions are from TAIR (http://www.arabidopsis.org/index.jsp).
RPKM, reads per gene kilobase per million reads.

Development (2014) doi:10.1242/dev.104687

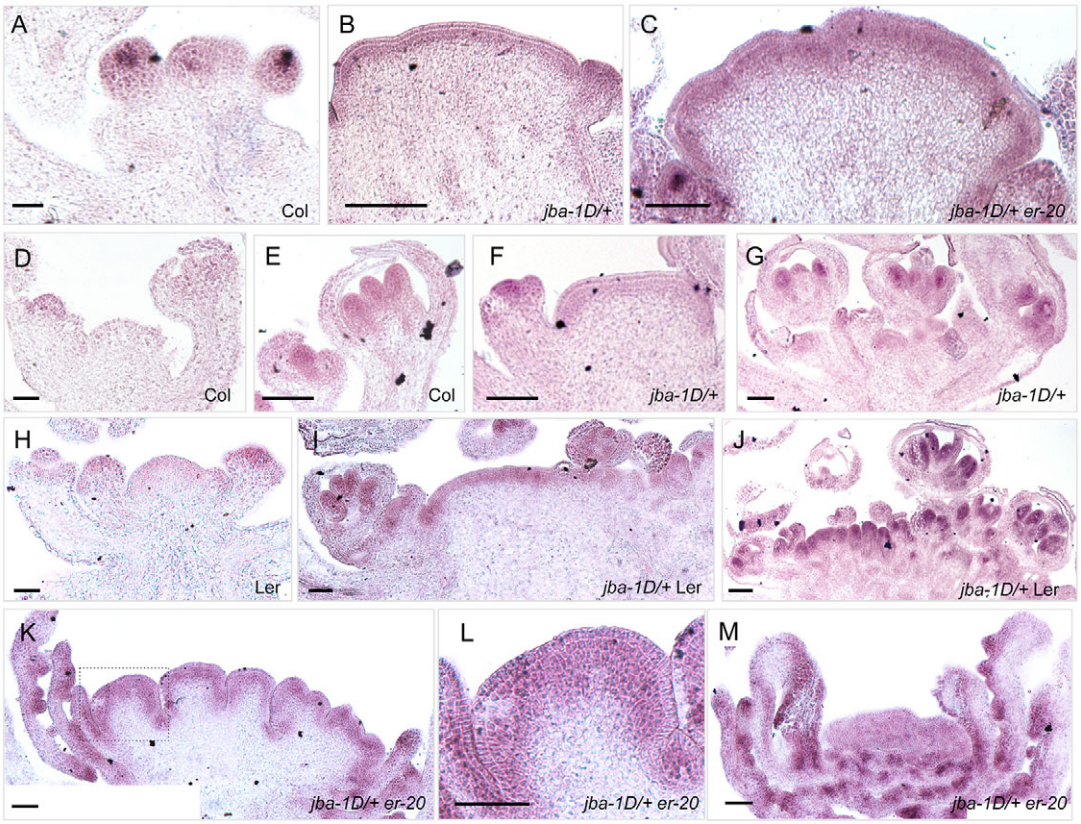

Fig. 4. Ectopic *WUS* and *AG* expression in *jba-1D/+er-20* IM. Inflorescence tissues hybridized (purple staining) with a (A-C) *WUS* antisense or an (D-M) *AG* antisense RNA probe. (A,D,E) Col IM and flower primordia. (H) L*er* inflorescence. (B,C) Ectopic *WUS* expression in the outer layers throughout *jba-1D/+* and *jba-1D/+er-20* IMs. (F) Weak *AG* signal in the three uppermost cell files of the *jba-1D/+* IM. (G) *AG* expression in *jba-1D/+* floral primordia. (I,J) Strong *AG* expression in *jba-1D/+* L*er* floral primordia and in the three or four uppermost cell files of the IM. (K-M) Ectopic *AG* expression in *jba-1D/+er-20* IMs. Intense *AG* signal in the four outer cell layers of the splitting IMs, as well as in the adaxial region of the ectopic carpels and in their ovules. (L) Magnified view of the boxed area in K. Scale bars: 50 µm.

(Fig. 5C). The *er-2* allele is an X-ray-induced frameshift mutation (Hall et al., 2007). *jba-1D/+er-2* IMs showed the same ectopic carpel formation phenotype as *jba-1D/+er-20* IMs (Fig. 5D,E). These results indicate that loss of *ER* function is responsible for the *jba-1D/+* modifier phenotypes.

The *ER* genes redundantly regulate SAM function (Shpak et al., 2004; Uchida et al., 2013). Therefore, we asked whether *ERL1* upregulation in *jba-1D/+er-20* IMs partially compensates for the mutation in *ER*. We generated triple mutants by crossing *jba-1D/+er-20* to the *erl1*-null mutant (SALK_081669) and observed two types of enhancement according to the *jba-1D* background (hemi-or homozygous) (Fig. 5F-J). In *jba-1D er-20 erl1* plants, the ectopic carpels are evident after only four or five normal flowers have formed (Fig. 5F-H). *jba-1D/+ er-20 erl1* plants display enhanced fasciation of the stems, which appear to be flattened with more multi-fused carpels, suggesting the presence of an enlarged wider IM (Fig. 5I,J). Consistent with the expression of *ER* genes in the shoot apex (Shpak et al., 2004; Uchida et al., 2013; Yokoyama et al., 1998), these results implicate the ER family members in IM size regulation.

The *ER* gene regulates meristem development in a *CLV*-independent pathway

Several *er* mutations enhance the SAM enlargement and gynoecium phenotypes of the CLV pathway mutants (Durbak and Tax, 2011). To test whether the *er-20* mutation acts in the CLV pathway, we generated *jba-1D/+er-20 clv3-2* plants (Fig. 6). Compared with wild-type Col and L*er* (Fig. 6A,B) inflorescences, both *clv3-2*-null and *jba-1D/+er-20* inflorescences are enlarged and produce supernumerary flowers (Fig. 6C,E,L). *jba-1D/+er-20 clv3-2* plants, however, form enormously enlarged IMs that produce few flowers before shifting to carpel formation at the periphery (Fig. 6G,M). The huge IM gradually increases in size and the multi-fused carpel structure keeps growing even 14 weeks after bolting (Fig. 6O). This synergistic interaction between *clv3-2* and *jba-1D/+er-20* indicates that *CLV3, HD-ZIPIII* and *ER* regulate SAM size in separate genetic pathways (supplementary material Fig. S6).

The *jba-1D/+er-20 clv3-2* gynoecium phenotypes also show a synergistic effect. Wild-type, *jba-1D/+* and *jba-1D/+er-20* gynoecia consist of two fused carpels, whereas *clv3-2* gynoecia are composed of four to six carpels (Fig. 6H). *jba-1D/+er-20 clv3-2* gynoecia are short and consist of 10 to 14 carpels, causing the fruit to have a sphere-like appearance (Fig. 6H,I). Because carpel number is tightly associated with FM size (Clark et al., 1993), these results indicate a direct role for ER in FM size regulation. In wild-type plants, stem cell termination in the FM is tightly coupled to the formation of carpel primordia, resulting in a mature gynoecium with two fused carpels (Fig. 6H) (Lenhard et al., 2001). By contrast, *jba-1D/+er-20 clv3-2* flowers not only form multi-carpel gynoecia, but their FMs fail to terminate and continue to produce numerous additional carpels, causing the gynoecia to burst (Fig. 6J,K). Thus, each *jba-1D/+er-20 clv3-2* gynoecium develops into a structure that

Development (2014) doi:10.1242/dev.104687

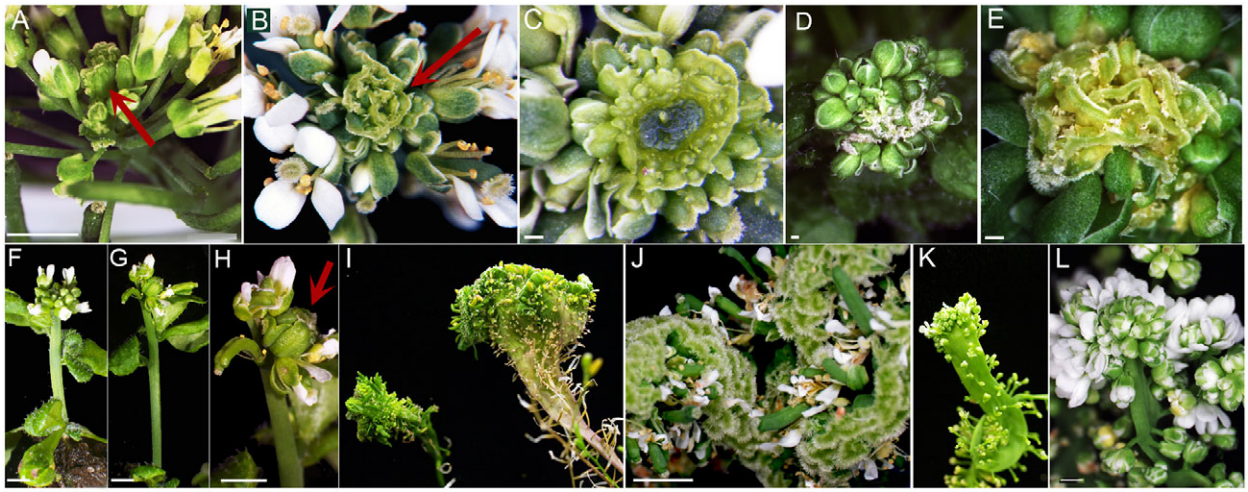

Fig. 5. Genetic interactions between *jba-1D/+, jba-1D/+er-20* and *ER* family mutants. (A-C) *jba-1D/+* crossed to L*er* exhibiting multi-fused carpels (red arrows) (A,B) or enlarged IM with concentric ring of carpels (C). (D,E) *jba-1D/+* Col *er-2* plants display whorls of multifused carpels within carpels. (F-H) *jba-1D er-20 erl1* plant 2 weeks after bolting. (F) *jba-1D er-20* inflorescence (G,H) *jba-1D er-20 erl1* inflorescence exhibits ectopic carpel formation (red arrow). (I,J) *jba-1D/+er-20 erl1* plant exhibits an extremely fasciated stem. (I) *jba-1D/+er-20* (left) and *jba-1D/+er-20 erl1* (right). (J) *jba-1D/+er-20 erl1* enhanced multi-fused carpel structure. (K,L) *jba-1D/+er-20 ag-1* plants display extremely fasciated stems that generate supernumerary flowers composed entirely of sepals and petals. Scale bars: 2 mm in A,F-H,J; 1 mm in L; 250 µm in C-E.

resembles the multifused carpel structure of the *jba-1D/+er-20* IM. These gynoecium phenotypes are consistent with a role for ER in regulating FM size and FM termination through a separate genetic pathway from the CLV pathway.

DISCUSSION

In this study we show that interference with SAM homeostasis between cell proliferation and cell recruitment for lateral organ formation by reducing *HD-ZIPIII* and *ER* gene function results in abnormal development, characterized by phyllotaxis alteration at the vegetative stage and ectopic carpel formation at the reproductive stage.

ER regulates *WUS* transcription and vegetative phyllotaxis

The *ER* gene is expressed in the SAM and throughout the FM at stages 1-3 (Roeder and Yanofsky, 2006; Shpak et al., 2004; Uchida

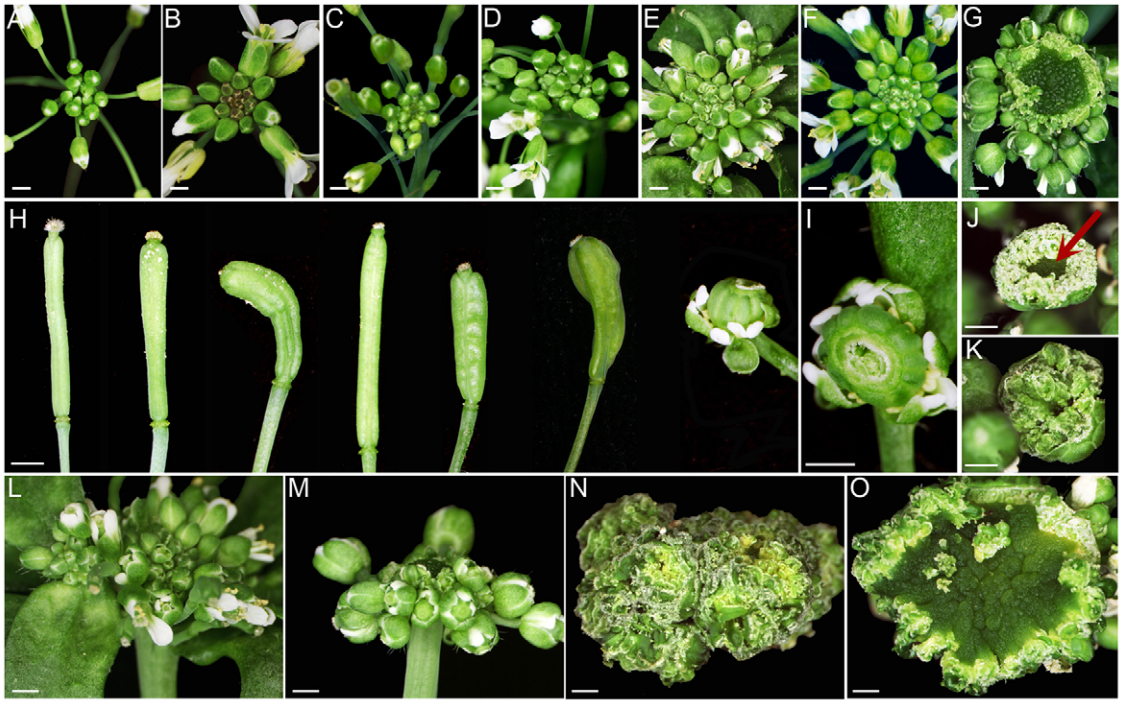

Fig. 6. Genetic interactions between *jba-1D/+er-20* and *clv3* plants. (A-G) Top view of inflorescences 2 weeks after bolting. (A) Col, (B) L*er*, (C) *clv3-2*, (D) *jba-1D/+*, (E) *jba-1D/+er-20*, (F) *jba-1D/+ clv3-2* and (G) *jba-1D/+er-20 clv3-2* plants display huge meristems. (H) Gynoecia from the same genotypes as A-G in the same order. (I-K) Short sphere-shaped *jba-1D/+er-20 clv3-2* gynoecia (I) at an early stage containing 12 valves, (J) with an indeterminate floral meristem (red arrow) producing numerous carpels and (K) bursting due to prolonged meristem activity that continuously produces carpels. (L-O) Side views of *jba-1D/+er-20* (L,N) and *jba-1D/+ er-20 clv3-2* (M,O) plants at 2 (L,M) and 14 (N,O) weeks after bolting. Scale bars: 1 mm.

Development (2014) doi:10.1242/dev.104687

et al., 2013; Yokoyama et al., 1998). Here, we show that *jba-1D/+* plants carrying a mutation in *ER* develop enormous SAMs that are wider and taller than *jba-1D/+* meristems, and contain more cells. These data fit with previous work showing that mutations in *ER* enhance meristem-derived phenotypes (Diévart et al., 2003; Durbak and Tax, 2011; Uchida et al., 2013). An increase in meristem size can occur via several pathways: a higher rate of cell division within the meristem, an increase in the size of the stem cell reservoir due to expansion of the OC that specifies their identity, or an accumulation of meristematic cells at the SAM periphery due to reduced cell incorporation into organ primordia (Kirch et al., 2003; Laufs et al., 1998b; Seidlová, 1980). The *ER* genes play overlapping roles in promoting cell proliferation in stems, leaves and floral organs (Torii et al., 1996; Shpak et al., 2003). If ER has the same function in the SAM, then mutations in *ER* should lead to a reduction SAM cell number. However, we observe that loss of *ER* activity in *jba-1D/+* leads to a dramatic increase in SAM size and cell number (Figs 1,3,4; supplementary material Fig. S1), suggesting that ER does not directly promote cell division in the SAM.

In *jba-1D* plants, a reduction in *HD-ZIPIII* transcript levels results in *WUS* upregulation and expression domain expansion (Williams et al., 2005). The *er*-20 mutation causes a further significant increase in *WUS* transcript levels, revealing a function for ER as a negative regulator of *WUS* expression. Furthermore, the enlarged *jba-1D/+er-20* SAM produces supernumerary organ primordia, indicating that the increase in meristem size is not due to a reduced rate of primordium initiation but is the result of defective ER regulation of *WUS*.

It has been suggested that meristem size could have a major influence on phyllotaxis (Bainbridge et al., 2008). Our observations that *jba-1D/+er-20* plants have extremely enlarged SAMs from which four primordia initiate simultaneously demonstrates the impact of meristem size on phyllotactic pattern. An accepted model for controlling phyllotaxis is that new primordia initiate at auxin maxima points on the SAM periphery (Benková et al., 2003; Heisler et al., 2005; Vanneste and Friml, 2009). Once an auxin maximum forms, it depletes auxin from the adjacent cells, resulting in the formation of a new auxin maximum, and therefore the emergence of a new primordium, only at a maximal distance from the established organs (Berleth et al., 2007; Lohmann et al., 2010; Reinhardt et al., 2003). In wild-type *Arabidopsis* plants, single auxin maxima form sequentially, resulting in a spiral phyllotaxis. In *er-20* plants there is no alteration in phyllotaxis, indicating that ER on its own does not regulate leaf primordia initiation. We therefore propose that the increased surface of *jba-1D/+er-20* vegetative meristems provides adequate distances to allow four auxin maxima to develop simultaneously (Fig. 1N), and that an increase in meristematic cells enables the SAM periphery to supply a sufficient number of founder cells to initiate extra organ primordia.

This idea is consistent with the elevated expression levels of the *GH3.3* early auxin-responsive gene in *jba-1D/+er-20* plants, which implies that additional auxin is present to stimulate its transcription. In conclusion, our observations indicate that ER negatively regulates *WUS* transcription, such that loss of ER function in the *jba-1D/+* background leads to a massive increase in SAM size that affects phyllotaxis rather than to direct regulation of primordia initiation.

ER and *HD-ZIPIII* genes link SAM size maintenance with floral meristem identity specification

Upon bolting, the fasciated *jba-1D/+er-20* IMs produce numerous normal flowers until a cell fate switch occurs at the IM periphery, leading to ectopic carpel formation. Two important questions raised are why does this cell identity switch occur, and why does it take place around 4 weeks after bolting rather than exactly at the reproductive transition? Because the phenotype occurs in the context of high levels of ectopic *WUS* and *AG* mRNA expression across the IMs, which is more dramatic in *jba-1D/+er-20* than in *jba-1D/+*, we propose that it is a matter of reaching a threshold of *AG* ectopic expression during inflorescence development.

In wild-type FMs, *AG* transcription is activated at stage 3 by WUS and LEAFY (Hong et al., 2003). In both *jba-1D/+* and *jba-1D/+er-20* plants, the inflorescence stems gradually increase in width (supplementary material Fig. S1), indicating a progressively enlarging IM as a result of a gradual increase in the size of the *WUS* expression domain (Fig. 4). A similar gradual increase in *WUS* expression is detected in CLV mutants during their development (Clark et al., 1993; Würschum et al., 2006). In *jba-1D/+* plants, *WUS* is upregulated to a level that leads to *AG* ectopic activation across the IM (Fig. 4), yet the amount of *AG* mRNA is not sufficient to induce a switch from FM to carpel identity. We propose that once *jba-1D/+er-20* plants bolt, *WUS* mRNA levels are high enough to activate *AG* across the IM, but not to the level required for carpel specification. During the next 4 weeks, *WUS* and *AG* expression continues to increase throughout the *jba-1D/+er-20* IMs (Figs 2,4; Table 1), with the gradual increase in *WUS* transcription ultimately inducing sufficient *AG* ectopic expression to surpass a threshold that triggers carpel formation.

Consistent with this concept, early studies indicate that AG likely functions in a dose-dependent fashion (Mizukami and Ma, 1995). In addition, in *35S::AG* lines that constitutively express *AG*, the development of carpeloid structures correlates with high levels of *AG* expression, whereas lines with low levels of *AG* transcription show no visible phenotypes (C.C.C. and J.C.F., unpublished). This model is also consistent with evidence from *jba-1D er-20 erl1* and *jba-1D/+er-20 clv3-2* plants, in which the IMs form ectopic carpels much earlier. The meristems of these mutants appear larger than those of *jba-1D/+er-20* plants, implying that *WUS* transcript levels are higher, as they are in *er erl1 erl2* meristems (Uchida et al., 2013). We propose that in the triple mutant IMs, the extremely elevated *WUS* transcription levels leads to the activation of *AG* to the required threshold much earlier than in *jba-1D/+er-20* IMs, and therefore to the appearance of ectopic carpels shortly after bolting.

Although *AG* is expressed in the upper cell layers across the *jba-1D er-20* IM, ectopic carpel initiation is restricted to the periphery. One possible explanation for this is the presence of factors that specify pluripotent fate and preventing cell differentiation at the SAM center. These factors would be absent or inhibited at the periphery, allowing cell differentiation and thus permitting AG function to promote carpel formation. Supporting evidence is the phenotype of *jba-1D/+er-20 clv3-2* plants, which exhibit gigantic IMs with reduced ectopic carpel formation at the periphery. Mutations in *CLV3* result in *WUS* domain expansion and a consequent increase in stem cell accumulation in shoot and floral meristems (Brand et al., 2000). We propose that in *jba-1D/+er-20 clv3-2* IMs, homeostasis is shifted towards stem cell identity, leaving fewer cells with the ability to differentiate. As a consequence, the triple mutant has a gigantic meristem with fewer carpeloid structures. Another explanation may be that other factors necessary for AG-mediated specification of carpel identity are absent from the center of the SAM. The need for additional factors is consistent with overexpression studies showing that ectopic *AG* activation is not sufficient to fully induce gynoecium formation outside of the flower (Lenhard et al., 2001; Mizukami and Ma, 1992), and with mutants such as *clf* in which ectopic *AG* expression in leaves does not cause ectopic gynoecium formation (Goodrich et al., 1997; Laufs et al., 1998b).

Development (2014) doi:10.1242/dev.104687

Our results indicate that ER and the *miR166g*-regulated *HD-ZIPIII* genes play an indirect role in specifying *Arabidopsis* FM identity. By negatively regulating *WUS* levels and restricting the *WUS* domain they prevent ectopic *AG* activation across the inflorescence meristem after the transition to flowering. This in turn enables the specification of floral meristem identity and precludes a switch to carpel cell identity on the IM flanks. Consistent with our data, a recent study (Bemis et al., 2013) independently confirms a function for the *ER* family genes in flower meristem development.

ER plays a role in meristem regulation independently from the CLV pathway

jba-1D/+ gynoecia have two carpels with no detectable fifth whorl, indicating that FM size is not significantly increased and FM termination is unaffected. This suggests that repression of *WUS* expression in the center of the FM is not delayed in a *miR166g* overexpression background. The gynoecia of *jba-1D/+ er-20* flowers also show no morphogenetic defects, suggesting either that *ER* and the *HD-ZIPIII* genes play a minor role in regulating FM size and determinacy or that FM size and termination are more tightly controlled by other factors, such as CLV3 (Clark et al., 1997), than the SAM size.

jba-1D/+ er-20 clv3-2 plants show strong synergistic phenotypes in both the IMs and flowers. When these three pathways are non-functional, the plants exhibit severe phenotypes corresponding to four distinct morphological changes. The IMs display a macroscopic increase in size, with ectopic carpel formation around the periphery, the flowers form more carpels, and the *clv3-2* FM indeterminacy defect is enhanced. None of the single mutants or double mutant combinations shows any resemblance to the *jba-1D/+ er-20 clv3-2* flowers; therefore, we conclude that all three pathways have an important role in FM regulation. Because all of the *jba-1D/+ er-20 clv3-2* flower phenotypes can be explained by altered *WUS* expression, we conclude that the three factors – *miR166*, ER and CLV3 – regulate *WUS* transcription in the FM via different genetic pathways.

In conclusion, our work illustrates the delicate balance between stem cell specification and differentiation in the meristem, and shows that a shift from this balance leads not only to increased meristem size but also to abnormal phyllotaxy and reproductive development. We have identified a role for a second receptor kinase signaling pathway – the ER pathway – in *WUS* regulation, and therefore in SAM and FM size regulation, that acts independently of the CLV signaling pathway. In addition, we have determined that negative regulation of both the *WUS* expression domain and its transcription levels by the *ER* gene family and the *miR166g*-regulated *HD-ZIPIII* genes is associated with a shift from spiral to whorled leaf phyllotaxis and is required for proper specification of FM identity. Future studies are needed to determine the intracellular elements downstream of the ER receptor kinase that regulate *WUS* transcription. It will also be of great interest to identify the upstream ligand controlling this cascade.

MATERIALS AND METHODS

Growth conditions and plant materials

Plants were grown under long days (16 hours light/8 hours dark) and temperatures of 18-22°C, in soil or on Murashige and Skoog (MS) plates.

EMS mutagenesis of *jba-1D* seeds

EMS mutagenesis was performed as described previously (Jander et al., 2003). M2 seeds from pools of 50 M1 plants were planted and screened for modified *jba-1D* phenotypes.

Plant materials

The plant materials used in this study were: Columbia (Col-0), Landsberg *erecta* (L*er*), *jba-1D* (Williams et al., 2005), *clv3-2* (Brand et al., 2000), *ag-1* (SALK_014999), *er-2* (CS3401) and *erl1* (SALK_081669). Double mutants were generated by crossing *jba-1D/+* plants to L*er*, *clv3-2* and *er-2* plants, and by crossing *jba-1D/+ er-20* plants to *clv3-2* and *erl1* plants. Double mutant plants were identified phenotypically and by PCR genotyping the F2 progeny.

Construction of transgenic lines

A 9 kb genomic fragment corresponding to the *ER* promoter and gene, spanning from the 3′ end of the *ER* upstream gene to the 5′ UTR side of the *ER* downstream gene was amplified from *jba-1D/+* DNA, cloned into pENTR/D-TOPO (Invitrogen) and recombined into a modified pK2GW7 binary vector (Ghent University) using the Gateway LR Clonase enzyme (Invitrogen). Transgenic lines were generated by the Agrobacterium-mediated floral dip method (Clough and Bent, 1998) into *jba-1D/+ er-20* and selected on MS plates containing kanamycin to select for the *ER* transgene and glufosinate ammonium (Fluka 45520) to select for the *jba-1D* allele.

Microscopy and histology

Plant images were captured using an Olympus SZX7 Stereomicroscope. Scanning electron microscopy was performed as described previously (Bowman et al., 1989) using a Hitachi 4700 scanning electron microscope. For histology analyses, 9-day-old seedlings were fixed, embedded and sectioned as described previously (Carles et al., 2004), and stained in Toluidine Blue solution.

Quantitative RT-PCR analysis

Total RNA was isolated from 8-day-old seedlings growing on MS plates using the Qiagen RNeasy Mini-kit. cDNA synthesis was performed with the Invitrogen SuperScript II Reverse Transcriptase, using 1 µg of RNA. RT-qPCR analysis was carried out using a Rotor-Gene-Q-instrument (Qiagen), with Absolute-Blue-qPCR-SYBR-Green Mix (Thermo). Three biological replicates were used for each genotype and three independent technical replicates were performed for each cDNA sample. *ACTIN2* (AT3G18780) was used as control and relative expression analysis was calculated using the 2-ddCT method (Livak and Schmittgen, 2001). Statistical analysis was performed using JMP software (SAS Institute). Student's *t*-test was used for comparison of means (significantly different at $P<0.05$). Primers used for RT-qPCR analysis are as follows: *ACT2*-AT3G18780, GGATCTGTACGGTAACATTGTGC (forward) and CCACCGATCCAGACACTGTAC (reverse); *WUS*-AT2G17950, CCAGCTTCAATAACGGGAATTTAAATCATGCA (forward) and TCATGTAGCCATTAGAAGCATTAACAACACCACAT (reverse); *STM*-AT1G62360, GATAGGAACAATAATGGGTCATCCG (forward) and AACCACTGTACTTGCGCAAGAG (reverse); *GH3.3*-AT2G23170, GTCCGGTGCTCACGAGTTAT (forward) and ATGCTTTGGGATGAGTCTGG (reverse); *ER*-AT2G26330, AGACGGGGAACAATGAAGTG (forward) and GGTGCATAGGAGTGCCAGTT (reverse); *CLV3*-AT2G27250, GTTCAAGGACTTTCCAACCGCAAGATGAT (forward) and CCTTCTCTGCTTCTCCATTTGCTCCAACC (reverse); *ERL2*-AT5G07180, CGTCTCCACCTCCAAAGAAG (forward) and TCACGGAACTGAACAAACCA (reverse).

Differential expression analysis by mRNA-seq

Four weeks after bolting, 30 *jba-1D/+* and 30 *jba-1D/+ er-20* IMs were collected by immersing the IM in liquid nitrogen and detaching the FM under a stereomicroscope. Bare meristems were pooled and total RNA isolated using Qiagen RNeasy-Mini-kit. mRNA was used to prepare libraries using TruSeqTM-RNA and single-end sequencing was performed by multiplexing on Illumina Hiseq-2000 at the Technion Genome Center. Data analysis was carried out at the Bioinformatics-Core-Facility in Ben-Gurion University. Raw sequence reads (Fastq files) were quality assessed using the FastQC software, and then aligned to the *Arabidopsis* genome using TopHat (70M for *jba-1D/+* and 50M for *jba-1D/+ er-20*). TAIR10 Genome reference sequence and gene model annotations for TopHat analysis were obtained from Illumina iGenomes website (http://tophat.cbcb.umd.edu/

igenomes.html). Estimation of transcript and gene abundances in each sample as FPKM values (fragments per kilobase of exon per million fragments mapped) and differential expression analysis were carried out using CuffDiff (parameters –c 5 –b –u –M). Genes with $P<0.01$ and [fold of change]>2 (total of 3524 genes) were considered differentially expressed. Genes are annotated with TAIR AGI locus names ('TAIR genes').

In situ RNA hybridization

Inflorescences were harvested 4 weeks after bolting. Tissue fixation and *in situ* hybridization were performed as described previously (Seidlová, 1980). Probes were transcribed using a digoxigenin-labeling mix (Roche). *WUS* antisense probe was generated as described previously (Mayer et al., 1998). *AG* antisense probe was generated by T7 RNA polymerase activity from a 1 kb insert cloned into the pBS KS+ vector (Seidlová, 1980).

Acknowledgements

We thank Hanita Zemach (Volcani center) for technical assistance and the *Arabidopsis* Biological Resource Center for insertion lines.

Competing interests

The authors declare no competing financial interests.

Author contributions

L.E.W. developed the concepts, T.M., F.M. and Y.K. performed experiments, L.E.W. wrote the manuscript, C.C.C. and J.C.F. edited and prepared the manuscript prior to submission.

Funding

This work was supported by the Israel Science Foundation [1351/10 to T.M.], by Vaadia-BARD [IS-4336-10R to Y.K.], by the US Department of Agriculture [5335-21000-029-00D to J.C.F], by the Centre National de la Recherche Scientifique (CNRS Higher Education chair [position 0428-64 to C.C.C.] and by Alpes county [ADR Cluster 7, 12-01293101 to F.M.]. Deposited in PMC for immediate release.

Supplementary material

Supplementary material available online at
http://dev.biologists.org/lookup/suppl/doi:10.1242/dev.104687/-/DC1

References

Alvarez-Buylla, E. R., Benitez, M., Corvera-Poire, A., Chaos Cador, A., de Folter, S., Gamboa de Buen, A., Garay-Arroyo, A., Garcia-Ponce, B., Jaimes-Miranda, F., Perez-Ruiz, R. V., et al. (2010). Flower development. *Arabidopsis Book* **8**, e0127.

Bainbridge, K., Guyomarc'h, S., Bayer, E., Swarup, R., Bennett, M., Mandel, T. and Kuhlemeier, C. (2008). Auxin influx carriers stabilize phyllotactic patterning. *Genes Dev.* **22**, 810-823.

Becker, A. and Theissen, G. (2003). The major clades of MADS-box genes and their role in the development and evolution of flowering plants. *Mol. Phylogenet. Evol.* **29**, 464-489.

Bemis, S. M., Lee, J. S., Shpak, E. D. and Torii, K. U. (2013). Regulation of floral patterning and organ identity by Arabidopsis ERECTA-family receptor kinase genes. *J. Exp. Bot.* [Epub ahead of print] doi:10.1093/jxb/ert270.

Benková, E., Michniewicz, M., Sauer, M., Teichmann, T., Seifertová, D., Jürgens, G. and Friml, J. (2003). Local, efflux-dependent auxin gradients as a common module for plant organ formation. *Cell* **115**, 591-602.

Berleth, T., Scarpella, E. and Prusinkiewicz, P. (2007). Towards the systems biology of auxin-transport-mediated patterning. *Trends Plant Sci.* **12**, 151-159.

Bowman, J. L., Smyth, D. R. and Meyerowitz, E. M. (1989). Genes directing flower development in Arabidopsis. *Plant Cell* **1**, 37-52.

Bowman, J. L., Smyth, D. R. and Meyerowitz, E. M. (2012). The ABC model of flower development: then and now. *Development* **139**, 4095-4098.

Brand, U., Fletcher, J. C., Hobe, M., Meyerowitz, E. M. and Simon, R. (2000). Dependence of stem cell fate in Arabidopsis on a feedback loop regulated by CLV3 activity. *Science* **289**, 617-619.

Busch, M. A., Bomblies, K. and Weigel, D. (1999). Activation of a floral homeotic gene in Arabidopsis. *Science* **285**, 585-587.

Carles, C. C. and Fletcher, J. C. (2003). Shoot apical meristem maintenance: the art of a dynamic balance. *Trends Plant Sci.* **8**, 394-401.

Carles, C. C., Lertpiriyapong, K., Reville, K. and Fletcher, J. C. (2004). The ULTRAPETALA1 gene functions early in Arabidopsis development to restrict shoot apical meristem activity and acts through WUSCHEL to regulate floral meristem determinacy. *Genetics* **167**, 1893-1903.

Clark, S. E., Running, M. P. and Meyerowitz, E. M. (1993). CLAVATA1, a regulator of meristem and flower development in Arabidopsis. *Development* **119**, 397-418.

Clark, S. E., Williams, R. W. and Meyerowitz, E. M. (1997). The CLAVATA1 gene encodes a putative receptor kinase that controls shoot and floral meristem size in Arabidopsis. *Cell* **89**, 575-585.

Clough, S. J. and Bent, A. F. (1998). Floral dip: a simplified method for Agrobacterium-mediated transformation of Arabidopsis thaliana. *Plant J.* **16**, 735-743.

Coen, E. S. and Meyerowitz, E. M. (1991). The war of the whorls: genetic interactions controlling flower development. *Nature* **353**, 31-37.

Colombo, M., Brambilla, V., Marcheselli, R., Caporali, E., Kater, M. M. and Colombo, L. (2010). A new role for the SHATTERPROOF genes during Arabidopsis gynoecium development. *Dev. Biol.* **337**, 294-302.

DeYoung, B. J., Bickle, K. L., Schrage, K. J., Muskett, P., Patel, K. and Clark, S. E. (2006). The CLAVATA1-related BAM1, BAM2 and BAM3 receptor kinase-like proteins are required for meristem function in Arabidopsis. *Plant J.* **45**, 1-16.

Diévart, A., Dalal, M., Tax, F. E., Lacey, A. D., Huttly, A., Li, J. and Clark, S. E. (2003). CLAVATA1 dominant-negative alleles reveal functional overlap between multiple receptor kinases that regulate meristem and organ development. *Plant Cell* **15**, 1198-1211.

Drews, G. N., Bowman, J. L. and Meyerowitz, E. M. (1991). Negative regulation of the Arabidopsis homeotic gene AGAMOUS by the APETALA2 product. *Cell* **65**, 991-1002.

Durbak, A. R. and Tax, F. E. (2011). CLAVATA signaling pathway receptors of Arabidopsis regulate cell proliferation in fruit organ formation as well as in meristems. *Genetics* **189**, 177-194.

Efroni, I., Blum, E., Goldshmidt, A. and Eshed, Y. (2008). A protracted and dynamic maturation schedule underlies Arabidopsis leaf development. *Plant Cell* **20**, 2293-2306.

Fletcher, J. C. (2001). The ULTRAPETALA gene controls shoot and floral meristem size in Arabidopsis. *Development* **128**, 1323-1333.

Furner, I. J. and Pumfrey, J. E. (1992). Cell fate in the shoot apical meristem of Arabidopsis-thaliana. *Development* **115**, 755-764.

Giulini, A., Wang, J. and Jackson, D. (2004). Control of phyllotaxy by the cytokinin-inducible response regulator homologue ABPHYL1. *Nature* **430**, 1031-1034.

Golz, J. F. and Hudson, A. (2002). Signalling in plant lateral organ development. *Plant Cell* **14 Suppl.**, S277-S288.

Gómez-Mena, C., de Folter, S., Costa, M. M., Angenent, G. C. and Sablowski, R. (2005). Transcriptional program controlled by the floral homeotic gene AGAMOUS during early organogenesis. *Development* **132**, 429-438.

Goodrich, J., Puangsomlee, P., Martin, M., Long, D., Meyerowitz, E. M. and Coupland, G. (1997). A Polycomb-group gene regulates homeotic gene expression in Arabidopsis. *Nature* **386**, 44-51.

Hall, M. C., Dworkin, I., Ungerer, M. C. and Purugganan, M. (2007). Genetics of microenvironmental canalization in Arabidopsis thaliana. *Proc. Natl. Acad. Sci. USA* **104**, 13717-13722.

Heisler, M. G., Ohno, C., Das, P., Sieber, P., Reddy, G. V., Long, J. A. and Meyerowitz, E. M. (2005). Patterns of auxin transport and gene expression during primordium development revealed by live imaging of the Arabidopsis inflorescence meristem. *Curr. Biol.* **15**, 1899-1911.

Hong, R. L., Hamaguchi, L., Busch, M. A. and Weigel, D. (2003). Regulatory elements of the floral homeotic gene AGAMOUS identified by phylogenetic footprinting and shadowing. *Plant Cell* **15**, 1296-1309.

Ito, T., Wellmer, F., Yu, H., Das, P., Ito, N., Alves-Ferreira, M., Riechmann, J. L. and Meyerowitz, E. M. (2004). The homeotic protein AGAMOUS controls microsporogenesis by regulation of SPOROCYTELESS. *Nature* **430**, 356-360.

Ito, T., Ng, K. H., Lim, T. S., Yu, H. and Meyerowitz, E. M. (2007). The homeotic protein AGAMOUS controls late stamen development by regulating a jasmonate biosynthetic gene in Arabidopsis. *Plant Cell* **19**, 3516-3529.

Jander, G., Baerson, S. R., Hudak, J. A., Gonzalez, K. A., Gruys, K. J. and Last, R. L. (2003). Ethylmethanesulfonate saturation mutagenesis in Arabidopsis to determine frequency of herbicide resistance. *Plant Physiol.* **131**, 139-146.

Jönsson, H., Heisler, M. G., Shapiro, B. E., Meyerowitz, E. M. and Mjolsness, E. (2006). An auxin-driven polarized transport model for phyllotaxis. *Proc. Natl. Acad. Sci. USA* **103**, 1633-1638.

Kaya, H., Shibahara, K. I., Taoka, K. I., Iwabuchi, M., Stillman, B. and Araki, T. (2001). FASCIATA genes for chromatin assembly factor-1 in arabidopsis maintain the cellular organization of apical meristems. *Cell* **104**, 131-142.

Kirch, T., Simon, R., Grünewald, M. and Werr, W. (2003). The DORNROSCHEN/ENHANCER OF SHOOT REGENERATION1 gene of Arabidopsis acts in the control of meristem ccll fate and lateral organ development. *Plant Cell* **15**, 694-705.

Krizek, B. A. and Fletcher, J. C. (2005). Molecular mechanisms of flower development: an armchair guide. *Nat. Rev. Genet.* **6**, 688-698.

Kwiatkowska, D. (2006). Flower primordium formation at the Arabidopsis shoot apex: quantitative analysis of surface geometry and growth. *J. Exp. Bot.* **57**, 571-580.

Laufs, P., Dockx, J., Kronenberger, J. and Traas, J. (1998a). MGOUN1 and MGOUN2: two genes required for primordium initiation at the shoot apical and floral meristems in Arabidopsis thaliana. *Development* **125**, 1253-1260.

Laufs, P., Grandjean, O., Jonak, C., Kiêu, K. and Traas, J. (1998b). Cellular parameters of the shoot apical meristem in Arabidopsis. *Plant Cell* **10**, 1375-1390.

Laux, T., Mayer, K. F., Berger, J. and Jürgens, G. (1996). The WUSCHEL gene is required for shoot and floral meristem integrity in Arabidopsis. *Development* **122**, 87-96.

Lease, K. A., Lau, N. Y., Schuster, R. A., Torii, K. U. and Walker, J. C. (2001). Receptor serine/threonine protein kinases in signalling: analysis of the erecta receptor-like kinase of Arabidopsis thaliana. *New Phytolog*, **151**, 133-143.

Lenhard, M., Bohnert, A., Jürgens, G. and Laux, T. (2001). Termination of stem cell maintenance in Arabidopsis floral meristems by interactions between WUSCHEL and AGAMOUS. *Cell* **105**, 805-814.

Leyser, H. M. O. and Furner, I. J. (1992). Characterisation of three shoot apical meristem mutants of Arabidopsis thaliana. *Development* **116**, 397-403.
Livak, K. J. and Schmittgen, T. D. (2001). Analysis of relative gene expression data using real-time quantitative PCR and the 2(-Delta Delta C(T)) Method. *Methods* **25**, 402-408.
Lohmann, D., Stacey, N., Breuninger, H., Jikumaru, Y., Müller, D., Sicard, A., Leyser, O., Yamaguchi, S. and Lenhard, M. (2010). SLOW MOTION is required for within-plant auxin homeostasis and normal timing of lateral organ initiation at the shoot meristem in Arabidopsis. *Plant Cell* **22**, 335-348.
Long, J. A. and Barton, M. K. (1998). The development of apical embryonic pattern in Arabidopsis. *Development* **125**, 3027-3035.
Long, J. A., Moan, E. I., Medford, J. I. and Barton, M. K. (1996). A member of the KNOTTED class of homeodomain proteins encoded by the STM gene of Arabidopsis. *Nature* **379**, 66-69.
Mallory, A. C., Bartel, D. P. and Bartel, B. (2005). MicroRNA-directed regulation of Arabidopsis AUXIN RESPONSE FACTOR17 is essential for proper development and modulates expression of early auxin response genes. *Plant Cell* **17**, 1360-1375.
Mayer, K. F., Schoof, H., Haecker, A., Lenhard, M., Jürgens, G. and Laux, T. (1998). Role of WUSCHEL in regulating stem cell fate in the Arabidopsis shoot meristem. *Cell* **95**, 805-815.
Medford, J. I., Behringer, F. J., Callos, J. D. and Feldmann, K. A. (1992). Normal and abnormal development in the arabidopsis vegetative shoot apex. *Plant Cell* **4**, 631-643.
Mizukami, Y. and Ma, H. (1992). Ectopic expression of the floral homeotic gene AGAMOUS in transgenic Arabidopsis plants alters floral organ identity. *Cell* **71**, 119-131.
Mizukami, Y. and Ma, H. (1995). Separation of AG function in floral meristem determinacy from that in reproductive organ identity by expressing antisense AG RNA. *Plant Mol. Biol.* **28**, 767-784.
Perales, M. and Reddy, G. V. (2012). Stem cell maintenance in shoot apical meristems. *Curr. Opin. Plant Biol.* **15**, 10-16.
Pinyopich, A., Ditta, G. S., Savidge, B., Liljegren, S. J., Baumann, E., Wisman, E. and Yanofsky, M. F. (2003). Assessing the redundancy of MADS-box genes during carpel and ovule development. *Nature* **424**, 85-88.
Reinhardt, D., Pesce, E. R., Stieger, P., Mandel, T., Baltensperger, K., Bennett, M., Traas, J., Friml, J. and Kuhlemeier, C. (2003). Regulation of phyllotaxis by polar auxin transport. *Nature* **426**, 255-260.
Roeder, A. H. and Yanofsky, M. F. (2006). Fruit development in Arabidopsis. *Arabidopsis Book* **4**, e0075.
Sablowski, R. (2004). Plant and animal stem cells: conceptually similar, molecularly distinct? *Trends Cell Biol.* **14**, 605-611.
Schoof, H., Lenhard, M., Haecker, A., Mayer, K. F., Jürgens, G. and Laux, T. (2000). The stem cell population of Arabidopsis shoot meristems in maintained by a regulatory loop between the CLAVATA and WUSCHEL genes. *Cell* **100**, 635-644.
Seidlová, F. (1980). The rate of cell-division in the shoot apical meristem during photoperiodic induction and transition to flowering. *Biol. Plant.* **22**, 428-433.
Shpak, E. D., Lakeman, M. B. and Torii, K. U. (2003). Dominant-negative receptor uncovers redundancy in the Arabidopsis ERECTA Leucine-rich repeat receptor-like kinase signaling pathway that regulates organ shape. *Plant Cell* **15**, 1095-1110.
Shpak, E. D., Berthiaume, C. T., Hill, E. J. and Torii, K. U. (2004). Synergistic interaction of three ERECTA-family receptor-like kinases controls Arabidopsis organ growth and flower development by promoting cell proliferation. *Development* **131**, 1491-1501.
Smith, R. S., Guyomarc'h, S., Mandel, T., Reinhardt, D., Kuhlemeier, C. and Prusinkiewicz, P. (2006). A plausible model of phyllotaxis. *Proc. Natl. Acad. Sci. USA* **103**, 1301-1306.
Smyth, D. R., Bowman, J. L. and Meyerowitz, E. M. (1990). Early flower development in Arabidopsis. *Plant Cell* **2**, 755-767.
Sussex, I. (1998). Themes in plant development. *Annu. Rev. Plant Physiol. Plant Mol. Biol.* **49**, xiii-xxii.
Takahashi, T., Matsuhara, S., Abe, M. and Komeda, Y. (2002). Disruption of a DNA topoisomerase I gene affects morphogenesis in Arabidopsis. *Plant Cell* **14**, 2085-2093.
Torii, K. U., Mitsukawa, N., Oosumi, T., Matsuura, Y., Yokoyama, R., Whittier, R. F. and Komeda, Y. (1996). The Arabidopsis ERECTA gene encodes a putative receptor protein kinase with extracellular leucine-rich repeats. *Plant Cell* **8**, 735-746.
Traas, J. (2013). Phyllotaxis. *Development* **140**, 249-253.
Uchida, N., Igari, K., Bogenschutz, N. L., Torii, K. U. and Tasaka, M. (2011). Arabidopsis ERECTA-family receptor kinases mediate morphological alterations stimulated by activation of NB-LRR-type UNI proteins. *Plant Cell Physiol.* **52**, 804-814.
Uchida, N., Shimada, M. and Tasaka, M. (2012). Modulation of the balance between stem cell proliferation and consumption by ERECTA-family genes. *Plant Signal. Behav.* **7**, 1506-1508.
Uchida, N., Shimada, M. and Tasaka, M. (2013). ERECTA-family receptor kinases regulate stem cell homeostasis via buffering its cytokinin responsiveness in the shoot apical meristem. *Plant Cell Physiol.* **54**, 343-351.
Vanneste, S. and Friml, J. (2009). Auxin: a trigger for change in plant development. *Cell* **136**, 1005-1016.
Vidaurre, D. P., Ploense, S., Krogan, N. T. and Berleth, T. (2007). AMP1 and MP antagonistically regulate embryo and meristem development in Arabidopsis. *Development* **134**, 2561-2567.
Vieten, A., Sauer, M., Brewer, P. B. and Friml, J. (2007). Molecular and cellular aspects of auxin-transport-mediated development. *Trends Plant Sci.* **12**, 160-168.
Wahl, V., Brand, L. H., Guo, Y. L. and Schmid, M. (2010). The FANTASTIC FOUR proteins influence shoot meristem size in Arabidopsis thaliana. *BMC Plant Biol.* **10**, 285.
Williams, L. and Fletcher, J. C. (2005). Stem cell regulation in the Arabidopsis shoot apical meristem. *Curr. Opin. Plant Biol.* **8**, 582-586.
Williams, L., Grigg, S. P., Xie, M., Christensen, S. and Fletcher, J. C. (2005). Regulation of Arabidopsis shoot apical meristem and lateral organ formation by microRNA miR166g and its AtHD-ZIP target genes. *Development* **132**, 3657-3668.
Wu, X., Dabi, T. and Weigel, D. (2005). Requirement of homeobox gene STIMPY/WOX9 for Arabidopsis meristem growth and maintenance. *Curr. Biol.* **15**, 436-440.
Würschum, T., Gross-Hardt, R. and Laux, T. (2006). APETALA2 regulates the stem cell niche in the Arabidopsis shoot meristem. *Plant Cell* **18**, 295-307.
Yanofsky, M. F., Ma, H., Bowman, J. L., Drews, G. N., Feldmann, K. A. and Meyerowitz, E. M. (1990). The protein encoded by the Arabidopsis homeotic gene agamous resembles transcription factors. *Nature* **346**, 35-39.
Yokoyama, R., Takahashi, T., Kato, A., Torii, K. U. and Komeda, Y. (1998). The Arabidopsis ERECTA gene is expressed in the shoot apical meristem and organ primordia. *Plant J.* **15**, 301-310.